Journal of
Mechanics of
Materials and Structures

THE EFFECTIVE THICKNESS OF LAMINATED GLASS PLATES

Laura Galuppi and Gianni Royer-Carfagni

Volume 7, No. 4 April 2012

mathematical sciences publishers

JOURNAL OF MECHANICS OF MATERIALS AND STRUCTURES
Vol. 7, No. 4, 2012

msp

THE EFFECTIVE THICKNESS OF LAMINATED GLASS PLATES

LAURA GALUPPI AND GIANNI ROYER-CARFAGNI

The flexural performance of laminated glass, a composite of two or more glass plies bonded together by polymeric interlayers, depends upon shear coupling between the glass components through the polymer. This effect is usually taken into account, in the design practice, through the definition of the *effective thickness*, i.e., the thickness of a monolith with equivalent bending properties in terms of stress and deflection. The traditional formulas *à la* Bennison–Wölfel are accurate only when the deformed bending shape of the plate is cylindrical and the plate response is similar to that of a beam under uniformly distributed load. Here, assuming approximating shape function for the deformation of laminated plates variously constrained at the edges, minimization of the corresponding strain energy furnishes new simple expressions for the effective thickness, which can be readily used in the design. Comparisons with accurate numerical simulations confirm the accuracy of the proposed simple method for laminated plates.

1. Introduction

Laminated glass is a sandwich structure where two or more glass plies are bonded together by thin polymeric interlayers with a process at high temperature and pressure in autoclave. Because of the shear deformability of the polymer, there is not a perfectly coupling between any two consecutive glass plies [Behr et al. 1993], and the degree of coupling depends upon the shear stiffness of the polymeric interlayer [Hooper 1973]. Consequently, the flexural response is somehow intermediate between the two borderline cases [Norville et al. 1998] of *layered limit*, i.e., frictionless relative sliding of the plies, and *monolithic limit*, i.e., perfect bonding of the plies. This problem has close similarities with the case of composite beams with partial interaction. The most classical contribution, conceived of for a concrete slab and a steel beam bonded by shear connectors, is associated with the name of Newmark et al. [1951], who considered a linear and continuous relationship between the relative interface slip and the corresponding shear stress. More recently Murakami [1984] introduced the usual hypotheses of Timoshenko beam to model the interlayer in the analysis of composite beams. In a recent paper, Xu and Wu [2007] presented a very comprehensive approach for static, dynamic and buckling behavior of composite beams with partial interaction, accounting for the influence of rotary inertia and shear deformation. Approximate formulations of this kind are particularly important for studying the problem of buckling of composite columns (e.g., [Le Grognec et al. 2012; Schnabl and Planinc 2011]), applicable to various materials, including lamellar wood [Cas et al. 2007].

Geometric nonlinearities are usually important because of the slenderness of the laminated panel [Aşik 2003], but are usually negligible when the loads are orthogonal to the panel surface and no in-plane forces are present. From an analytical point of view, it is often very difficult to obtain a closed-form solution for the strain and stress field in a laminated glass plate. An analytical approach has been recently proposed

Keywords: structural glass, laminated glass, composite structure, laminated plate, effective thickness, energy minimization.

by Foraboschi [2012] for the case of rectangular plates made of laminated glass, simply supported on four sides. The precise calculation of the resulting state of stress and strain is quite difficult and usually requires numerical analysis, complicated by the fact that response of the polymer is nonlinear, viscoelastic and temperature dependent [Behr et al. 1993; Bennison et al. 2005; Louter et al. 2010].

This is why simplified methods are becoming more and more popular in the design practice , and much of current research is directed towards their definition and verification [Foraboschi 2007]. Reference is made to [Ivanov 2006] for an updated list of the most relevant current literature.

A commonly accepted simplification is to assume that the polymer is linear elastic, with proper secant elastic moduli that account for environmental temperature and load duration. There are various commercial polymeric films: polyvinyl butyral (PVB), ethylene vinyl acetate (EVA), and sentry glass (SG) [Bennison et al. 2008; Bennison et al. 2001]. Depending upon the polymer type, temperature T and characteristic load-duration t_0, the secant shear modulus of the interlayer may vary from 0.01 MPa (PVB at $T = +60°\text{C}$ under permanent load) up to 300 MPa (SG at $T = 0°\text{C}$ and $t_0 = 1$ s). On the other hand, glass remains linear elastic up to failure (Young's modulus $E \simeq 70$ GPa and Poisson ratio $\nu \simeq 0.2$).

A simplified method of very practical value makes use the notion of "effective" thickness. This method has been introduced starting from the analysis for sandwich beams with linear elastic components originally developed by Wölfel [1987] and later transferred to the case of laminated glass [Bennison 2009; Calderone et al. 2009]. To illustrate, consider (as in Figure 1) a beam of length l and width b composed of two external glass plies of thickness h_1 and h_2 and Young's modulus E, bonded by a soft polymeric interlayer of thickness t and elastic shear modulus G. The latter has negligible axial and bending strength, but nevertheless it can transfer shear coupling stresses between the external layers. Let

$$A_i = h_i b, \quad I_i = \tfrac{1}{12} b h_i^3 \ \ (i = 1, 2), \quad H = t + \tfrac{1}{2}(h_1 + h_2), \quad A^* = \frac{A_1 A_2}{A_1 + A_2},$$
$$I_{\text{tot}} = I_1 + I_2 + A^* H^2, \quad A = bt, \quad B_s = E A^* H^2. \tag{1-1}$$

Clearly, I_{tot} is the cross sectional inertia of the composing glass layers properly spaced of the interlayer gaps, associated with the case of perfect bonding of the glass plies as in Bennison et al. [1999] (monolithic limit). Besides, B_s is the bending stiffness when the external layers have negligible inertia, while the mid-layer can only bear shear stress. When, as in the case of laminated glass, the external layers have

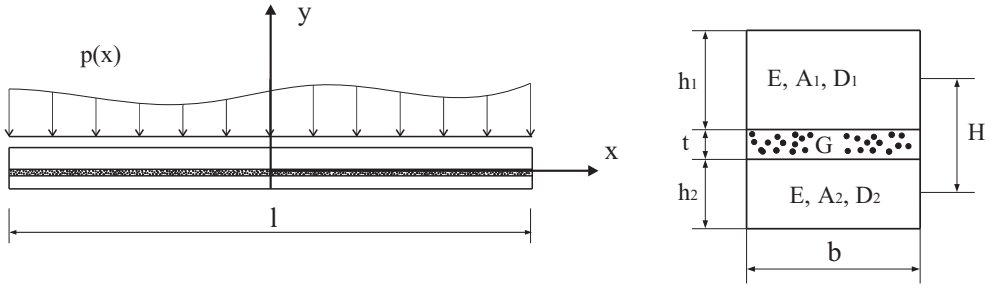

Figure 1. Beam composed of two glass plies bonded by a polymeric interlayer. Longitudinal and cross sectional view (not in the same scale).

nonnegligible inertia, Wölfel proposed the expression B_s^* defined as

$$B_s^* = EI_1 + EI_2 + \frac{1}{1+\mathcal{K}} B_s, \tag{1-2}$$

where the coefficient $(1+\mathcal{K})$ indicates the degradation of the bending properties of the composite due to the incomplete interaction between the external layers. Using the principle of virtual work one finds that the coefficient $\mathcal{K}$ is of the form

$$\mathcal{K} = \beta\, B_s \frac{\chi}{Gbtl^2}, \tag{1-3}$$

where, as explained in [Galuppi and Royer-Carfagni 2012], the shear coefficient of the intermediate layer χ is evaluated as $\chi = t^2/H^2$ and β is another parameter that depends upon the load condition. For simply supported beams, the corresponding values of β are recorded in [Wölfel 1987] for various loadings. Notice from (1-3) that $G \to \infty \Rightarrow \mathcal{K} \to 0$, so that from (1-2) also $B_s^* \to EI_{\text{tot}}$, i.e., the monolithic limit; moreover, $G \to 0 \Rightarrow \mathcal{K} \to \infty$ and $B_s^* \to E(I_1 + I_2)$, i.e., the layered limit.

Bennison [2009] and Calderone et al. [2009] have referred specifically to Wölfel's approach for the case of laminated glass. More precisely, they define the nondimensional coefficient $\Gamma = 1/(1+\mathcal{K})$, $\Gamma \in (0, 1)$, introduce the *equivalent moment of inertia* of the cross section in the form

$$I_{eq} = I_1 + I_2 + \Gamma \frac{A_1 A_2}{A_1 + A_2} H^2, \tag{1-4}$$

and consider for Γ the expression

$$\Gamma = \frac{1}{1+\beta \dfrac{\chi B_s}{Gbtl^2}} = \frac{1}{1+9.6\dfrac{tB_s}{GbH^2l^2}}. \tag{1-5}$$

This is equivalent to using in (1-3) the value $\beta = 9.6$, which corresponds to Wölfel's analysis for the particular case of a simply supported beam under uniformly distributed load. Consequently, recalling (1-4), for calculating the laminate deflection one can consider a monolithic beam with *deflection-effective thickness* $h_{\text{ef};w}$ given by

$$h_{\text{ef};w} = \sqrt[3]{h_1^3 + h_2^3 + 12\Gamma \frac{h_1 h_2}{h_1 + h_2} H^2}. \tag{1-6}$$

Once the deflection of the laminate is established, one can estimate the degree of connection offered by the deformable interlayer and, from this, the maximum stress in the glass can be easily estimated. The result [Bennison 2009; Calderone et al. 2009] is that the maximum bending stress in the i-th glass plies, $i = 1, 2$, is the same of that in a fictitious monolithic beam with analogous constraint and load conditions, with respectively *stress-effective thickness*

$$h_{1;\text{ef};\sigma} = \sqrt{\frac{h_{\text{ef};w}^3}{h_1 + 2\Gamma \dfrac{Hh_2}{h_1+h_2}}}, \quad h_{2;\text{ef};\sigma} = \sqrt{\frac{h_{\text{ef};w}^3}{h_2 + 2\Gamma \dfrac{Hh_1}{h_1+h_2}}}. \tag{1-7}$$

It is important to notice that this method relies upon the particular form of Γ given by (1-5), which assumes the coefficient $\beta = 9.6$, i.e., the one proposed by Wölfel for the very particular case of simply supported beams under uniformly distributed loading. Moreover, according to [Wölfel 1987], the validity of the method is limited because its simplifying assumptions are valid for statically determined composite beams, where the bending stiffness of the composite plies is considerably small. Nevertheless, this approach is widely used. In the design practice, the calculations for laminated glass panels are usually performed on an equivalent monolithic plate whose thickness is assumed to be given by (1-6), to determine maximum deflection, or by (1-7), where it is the bending stress to be calculated. This effective thickness is usually adopted in place of the actual thickness in analytic equations and simplified finite-element analysis; sometimes the method is abused in very delicate conditions, for example when calculating the stress concentrations around holes and contact regions in a neighborhood of the point-wise fixing of frameless glazing. In general, *no approach based upon the definition of the effective thickness can be used to evaluate local effects*. In any case, the Bennison–Wölfel method may lead to inaccurate results also when calculating maximum stress and deflection at the center of a laminated plate, especially when load and boundary conditions are different from that of a rectangular plate simply supported at two opposite side (cylindrical deformed shape) under uniformly distributed load.

In [Galuppi and Royer-Carfagni 2012] we treated the classical problem of a composite laminated glass beam under flexure using a variational approach similar in type to that proposed in [Aşik and Tezcan 2005] for numerical purposes. Using convenient shape functions for the beam deflection, simple formulas for the effective thickness were obtained which, for the one-dimensional case of beams with various constraint and load conditions, fitted with numerical experiments much better than the classical expressions (1-6) and (1-7). Our aim now is to extend this approach to the two-dimensional case of a rectangular laminated glass plate under uniform pressure, variously supported at the borders. For the cases considered in [Galuppi and Royer-Carfagni 2012] the problem is certainly much more complicated, but we show that by assuming again proper shape functions for the plate deflection, simple expressions of the effective thickness can be found. Comparisons with careful numerical experiments on full three-dimensional models, show the proposed formulation furnishes results more reliable than those obtainable with the classical Bennison–Wölfel approach. The method can be readily extended to plates of various shape, under diverse load conditions.

2. The variational problem

As indicated in Figure 2, with notation analogous to (1-1), consider a laminated plate composed of two glass layers of thickness h_1 and h_2 with Young's modulus E and Poisson's ratio ν, connected by a polymeric interlayer of thickness t and shear modulus G. Let

$$D_i = \frac{E h_i^3}{12(1-\nu^2)}$$

represent the flexural stiffness of the i-th glass plate, $i = 1, 2$, while H is the distance between their middle planes. Upon introduction of a reference system as indicated in Figure 2, the plate is identified by the $x - y$ domain Ω with border $\partial\Omega$, and is loaded by a pressure per unit area $p(x, y)$, not necessarily uniformly distributed.

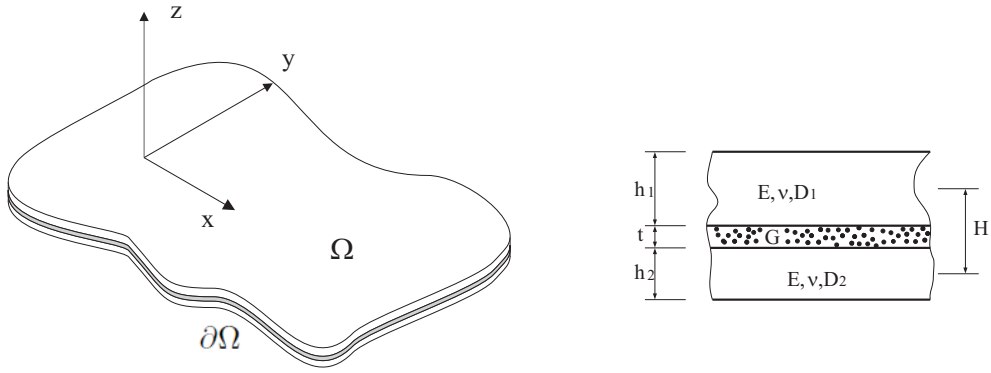

Figure 2. Plate composed of two glass plies bonded by a polymeric interlayer. Isometric and cross sectional view (not in the same scale).

No slippage is supposed to occur between glass and polymer (case of perfect bonding). Under the hypotheses that strains are small and rotations moderate, the kinematics is completely described by the out-of-plane displacement $w(x, y)$ in the z direction that, by neglecting the interlayer strain along z, is the same for the two glass layers, and the in-plane displacements of the i-th glass layers, $i = 1, 2$, for which the x and y components are denoted by $u_i(x, y)$ and $v_i(x, y)$, respectively (Figure 3).

2.1. ***The minimization problem.*** As represented Figure 3, let us denote with $u_{\text{sup}}(x, y)$ and $v_{\text{sup}}(x, y)$, $u_{\text{inf}}(x, y)$ and $v_{\text{inf}}(x, y)$, the x and y displacement components of those faces of the superior and inferior glass plies, respectively, in contact with the polymer. Then, the shear strain in the interlayer, constant through its thickness, is characterized by the components

$$\begin{aligned}\tilde{\gamma}_{zx} &= \frac{1}{t}[u_{\text{sup}}(x, y) - u_{\text{inf}}(x, y) + w_{,x}(x, y)t] = \frac{1}{t}[u_1(x, y) - u_2(x, y) + w_{,x}(x, y)H],\\ \tilde{\gamma}_{zy} &= \frac{1}{t}[v_{\text{sup}}(x, y) - v_{\text{inf}}(x, y) + w_{,y}(x, y)t] = \frac{1}{t}[v_1(x, y) - v_2(x, y) + w_{,y}(x, y)H],\end{aligned} \tag{2-1}$$

where subscript commas denote partial differentiation with respect to the indicated variable. The strain energy $\mathfrak{E}$ of the laminated glass plate is provided by the flexural and extensional contributions of the

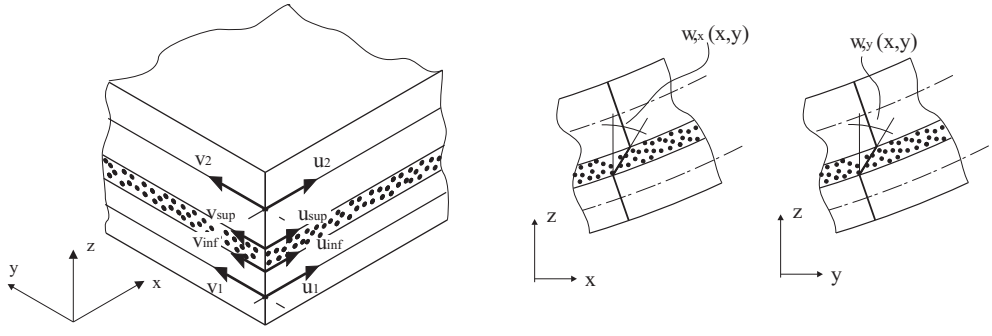

Figure 3. Relevant displacement components and corresponding deformation in the composite plate.

two glass layers, by the part corresponding to the shear deformation of the interlayer, and by the work associated with the external loads $p(x, y)$. We have, suppressing from the notation the dependence of w, u_i, v_i on x, y (see [Timoshenko and Woinowsky-Krieger 1971]):

$$\begin{aligned}\mathfrak{E}[w, u_1, u_2, v_1, v_2] = \int_\Omega \frac{1}{2}\Big\{&(D_1+D_2)[(w_{,xx}+w_{,yy})^2 - 2(1-\nu)(w_{,xx}w_{,yy} - w_{,xy}^2)]\\ &+ 12\frac{D_1}{h_1^2}\big[(u_{1,x}+v_{1,y})^2 - 2(1-\nu)\big(u_{1,x}v_{1,y} - \tfrac{1}{4}(u_{1,y}+v_{1,x})^2\big)\big]\\ &+ 12\frac{D_2}{h_2^2}\big[(u_{2,x}+v_{2,y})^2 - 2(1-\nu)\big(u_{2,x}v_{2,y} - \tfrac{1}{4}(u_{2,y}+v_{2,x})^2\big)\big]\\ &+ \frac{G}{t}\big[(u_1-u_2+w_{,x}\,H)^2 + (v_1-v_2+w_{,y}\,H)^2\big] + 2p(x,y)w\Big\}\,dx\,dy. \quad (2\text{-}2)\end{aligned}$$

The analysis of the first variation of the functional with respect to $w(x, y)$, $u_i(x, y)$ and $v_i(x, y)$, $i = 1, 2$, gives respectively the following Euler–Lagrange equations:

$$(D_1+D_2)\triangle\triangle w - \frac{GH}{t}[(u_1-u_2+w_{,x}\,H)_{,x} + (v_1-v_2+w_{,y}\,H)_{,y}] - p(x,y) = 0, \quad (2\text{-}3)$$

$$\frac{12D_1}{h_1^2}\Big(u_{1,xx} + \frac{1-\nu}{2}u_{1,yy} + \frac{1+\nu}{2}v_{1,xy}\Big) - \frac{G}{t}(u_1-u_2+w_{,x}\,H) = 0, \quad (2\text{-}4)$$

$$\frac{12D_2}{h_2^2}\Big(u_{2,xx} + \frac{1-\nu}{2}u_{2,yy} + \frac{1+\nu}{2}v_{2,xy}\Big) + \frac{G}{t}(u_1-u_2+w_{,x}\,H) = 0, \quad (2\text{-}5)$$

$$\frac{12D_1}{h_1^2}\Big(v_{1,yy} + \frac{1-\nu}{2}v_{1,xx} + \frac{1+\nu}{2}u_{1,xy}\Big) - \frac{G}{t}(v_1-v_2+w_{,y}\,H) = 0, \quad (2\text{-}6)$$

$$\frac{12D_2}{h_2^2}\Big(v_{2,yy} + \frac{1-\nu}{2}v_{2,xx} + \frac{1+\nu}{2}u_{2,xy}\Big) + \frac{G}{t}(v_1-v_2+w_{,y}\,H) = 0, \quad (2\text{-}7)$$

with conditions at the boundary $\partial\Omega$

$$\begin{aligned}\oint_{\partial\Omega}\Big\{(D_1+D_2)\frac{\partial}{\partial n}\triangle w - \frac{GH}{t}\big[(u_1-u_2+w_{,x}\,H),\, xn_x + (v_1-v_2+w_{,y}\,H),\, yn_y\big]\Big\}\,\delta w\,ds\\ - \oint_{\partial\Omega}(D_1+D_2)\big[(w_{,xx}+\nu w_{,yy})n_x + w_{,xy}\,n_y\big]\,\delta w_{,x}\;ds\\ - \oint_{\partial\Omega}(D_1+D_2)2(1-\nu)\big[w_{,xy}\,n_x + (w_{,xx}+\nu w_{,yy})n_y\big]\,\delta w_{,y}\;ds = 0, \quad (2\text{-}8)\end{aligned}$$

$$\oint_{\delta\Omega}\Big[(u_{i,x}+\nu v_{i,y})n_x + \frac{1-\nu}{2}(u_{i,y}+v_{i,x})n_y\Big]\,\delta u_i\,ds = 0,\ \ i = 1..2, \quad (2\text{-}9)$$

$$\oint_{\partial\Omega}\Big[\frac{1-\nu}{2}(u_{i,y}+v_{i,x})n_x + (v_{i,y}+\nu u_{i,x})n_y\Big]\,\delta v_i\,ds = 0,\ \ i = 1..2, \quad (2\text{-}10)$$

where $\delta w(x, y)$, $\delta u_i(x, y)$ and $\delta v_i(x, y)$ are the variations of $w(x, y)$, $u_i(x, y)$ and $v_i(x, y)$, $i = 1, 2$, respectively. As customary in the calculus of variations [Sagan 1969], the geometric constraints at the border furnish restriction on the possible variations of the displacement components. Then, (2-8), (2-9) and (2-10) give the boundary conditions for the problem at hand.

2.2. ***Interpretation of the Euler–Lagrange Equation and boundary conditions.*** With standard notation from plate theory [Timoshenko and Woinowsky-Krieger 1971], the x- and y-components of the in-plane forces-per-unit-length in the i-th glass ply are of the form

$$N_{ix} = \frac{12D_i}{h_i^2}(u_{i,x} + \nu v_{i,y}), \quad N_{iy} = \frac{12D_i}{h_i^2}(v_{i,y} + \nu u_{i,x}), \quad N_{ixy} = \frac{12D_i}{h_1^2}\frac{1-\nu}{2}(u_{i,y} + v_{i,x}). \tag{2-11}$$

As shown in Figure 4, imagine cutting the interlayer of the laminated plate with a plane parallel to x and y at an arbitrary height t^*. The tangential stress component on the resulting surfaces are $\tilde{\tau}_{zx} = G\tilde{\gamma}_{zx}$ and $\tilde{\tau}_{zy} = G\tilde{\gamma}_{zy}$, where the shear strains $\tilde{\gamma}_{zx}$ and $\tilde{\gamma}_{zy}$ have been defined in (2-1). Since $\tilde{\gamma}_{zx}$ and $\tilde{\gamma}_{zy}$ do not depend on z, $\tilde{\tau}_{zx}$ and $\tilde{\tau}_{zy}$ are independent of t^*. It is then easily verified that (2-4), (2-5), (2-6) and (2-7) are the equilibrium equations in the x and y directions of the composing glass plies, that is,

$$\begin{aligned} &N_{1x,x} + N_{1xy,y} + \tilde{\tau}_{zx} = 0, \quad N_{2x,x} + N_{2xy,y} - \tilde{\tau}_{zx} = 0, \\ &N_{1y,y} + N_{1xy,x} + \tilde{\tau}_{zy} = 0, \quad N_{2y,y} + N_{2xy,x} - \tilde{\tau}_{zy} = 0. \end{aligned} \tag{2-12}$$

Moreover, from the moment-curvature relationships [Timoshenko and Woinowsky-Krieger 1971] for the i-th glass plate,

$$M_{ix} = -D_i(w_{,xx} + \nu w_{,yy}), \quad M_{iy} = -D_i(w_{,yy} + \nu w_{,xx}), \quad M_{ixy} = D_i(1-\nu)(w_{,xy}), \tag{2-13}$$

one finds that Equation (2-3) can be rewritten as

$$(M_{1x} + M_{2x})_{,xx} + (M_{1y} + M_{2y})_{,yy} - 2(M_{1xy} + M_{2xy})_{,xy} - (\tilde{\tau}_{zx,x} + \tilde{\tau}_{zy,y})H - p = 0. \tag{2-14}$$

Notice from Figure 4 that the shear stress at the surfaces resulting after the horizontal cut of the interlayer are statically equivalent, for each one of the component glass plies, to distributed torques per unit length. In particular, $\tilde{\tau}_{zx}$ generates $m_{1zx}(x, y) = -\tilde{\tau}_{zx}(\frac{1}{2}h_1 + t - t^*)$ and $m_{2zx}(x, y) = -\tilde{\tau}_{zx}(\frac{1}{2}h_2 + t^*)$ in the upper and lower glass plate, respectively. Then, the overall torque per unit length on the two glass plates is $m_{zx}(x, y) = m_{1zx}(x, y) + m_{2zx}(x, y) = -\tilde{\tau}_{zx}(\frac{1}{2}(h_1 + h_2) + t) = -G\tilde{\gamma}_{zx}H$. Similarly, $\tilde{\tau}_{zy}$

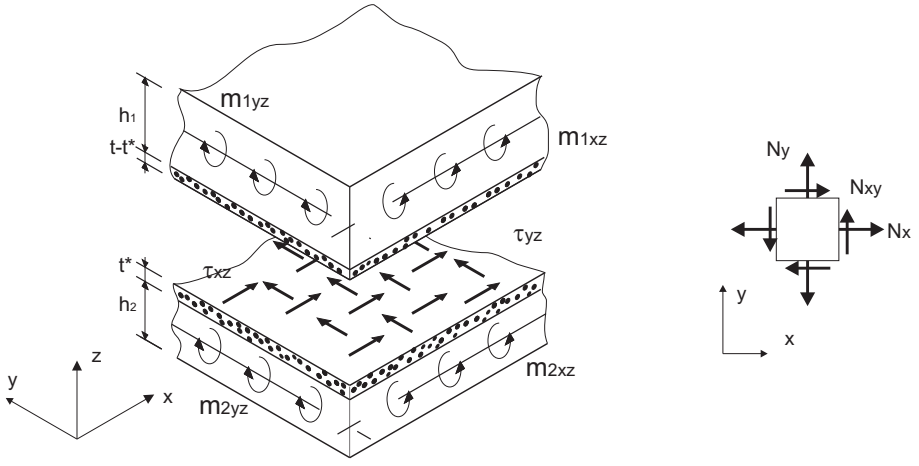

Figure 4. Equilibrium of portions of the laminated plate.

generates $m_{zy}(x, y) = -\tilde{\tau}_{zy}(\frac{1}{2}(h_1 + h_2) + t) = -G\tilde{\gamma}_{zy}H$. Henceforth, condition (2-3), or equivalently (2-14), represents the flexural equilibrium of the package glass + polymer under bending, in the form $(D_1 + D_2)\triangle\triangle w - p + m_{zx,x} + m_{zy,y} = 0$.

For what the border is concerned, (2-11) allows to write (2-9) and (2-10) in the form

$$\oint_{\partial\Omega} (N_{ix}n_x + N_{ixy}n_y)\delta u_i \, ds = 0, \quad \oint_{\partial\Omega} (N_{ixy}n_x + N_{iy}n_y)\delta v_i \, ds = 0 \quad (i = 1, 2), \tag{2-15}$$

these being the standard in-plane boundary conditions for the i-th glass layers [Timoshenko and Woinowsky-Krieger 1971]. Moreover, using (2-13) and defining $M_x = (M_{1x} + M_{2x})$, $M_y = (M_{1y} + M_{2y})$, $M_{xy} = (M_{1xy} + M_{2xy})$, condition (2-8) may be rearranged as

$$\oint_{\partial\Omega} [(M_{x,x} - M_{xy,y} - H\tilde{\tau}_{zx,x})n_x + (M_{y,y} - M_{xy,x} - H\tilde{\tau}_{zy,y})n_y]\,\delta w \, ds + \oint_{\partial\Omega} [M_x n_x + M_{xy}n_y]\,\delta w_{,x} \, ds + \oint_{\partial\Omega} [M_y n_y + M_{xy}n_x]\,\delta w_{,y} \, ds = 0. \tag{2-16}$$

This is readily interpretable because $Q_x = M_{x,x} - M_{xy,y}$ and $Q_y = M_{y,y} - M_{xy,x}$ represent the sum of the transversal shearing forces per unit length acting on the two glass plies. As in classical Kirchhoff plate theory [Timoshenko and Woinowsky-Krieger 1971], (2-16) gives the boundary condition in terms of bending couples and transversal shear.

2.3. ***Correlation between the displacements of the external layers.*** There are noteworthy identities, important for the forthcoming considerations, that correlate the displacements of the two constituent glass plies. In fact, we will prove that the (weighted) average displacement fields, defined as

$$U(x, y) = u_1(x, y) + \frac{h_2}{h_1} u_2(x, y), \quad V(x, y) = v_1(x, y) + \frac{h_2}{h_1} v_2(x, y), \tag{2-17}$$

are identically zero.

To illustrate, notice first that equations (2-4), (2-5), (2-6) and (2-7) may be rearranged in the form

$$\frac{12D_1}{h_1^2}\Big(u_{1,xx} + \frac{1-\nu}{2}u_{1,yy} + \frac{1+\nu}{2}v_{1,xy}\Big) = -\frac{12D_2}{h_2^2}\Big(u_{2,xx} + \frac{1-\nu}{2}u_{2,yy} + \frac{1+\nu}{2}v_{2,xy}\Big), \tag{2-18}$$

$$\frac{12D_1}{h_1^2}\Big(v_{1,yy} + \frac{1-\nu}{2}v_{1,xx} + \frac{1+\nu}{2}u_{1,xy}\Big) = -\frac{12D_2}{h_2^2}\Big(v_{2,yy} + \frac{1-\nu}{2}v_{2,xx} + \frac{1+\nu}{2}u_{2,xy}\Big). \tag{2-19}$$

In terms of $U(x, y)$ and $V(x, y)$, these can be rewritten as

$$\begin{aligned} U_{,xx} + \tfrac{1}{2}(1-\nu)U_{,yy} + \tfrac{1}{2}(1+\nu)V_{,xy} &= 0, \\ V_{,yy} + \tfrac{1}{2}(1-\nu)V_{,xx} + \tfrac{1}{2}(1+\nu)U_{,xy} &= 0, \end{aligned} \tag{2-20}$$

which is a system of partial differential equations defined on a connected domain Ω. If the glass plies are constrained so that $u_i = v_i = 0$, $i = 1..2$, on the boundary $\partial\Omega$, then from (2-17) also $U = V = 0$ on $\partial\Omega$. In general, however, the in-plane displacements of laminated glass are not constrained; in this case,

from (2-9) and (2-10) one finds the boundary conditions

$$\begin{aligned}(U_{,x}+\nu V_{,y})n_x+\tfrac{1}{2}(1-\nu)(U_{,y}+V_{,x})n_y=0 \quad \text{on } \partial\Omega,\\ \tfrac{1}{2}(1-\nu)(U_{,y}+V_{,x})n_x+(V_{,y}+\nu V_{,x})n_y=0 \quad \text{on } \partial\Omega.\end{aligned} \tag{2-21}$$

We can prove that the system of partial differential equations (2-20) with boundary condition $U = V = 0$ on $\partial\Omega$ or, equivalently, with boundary condition given by (2-21), implies $U = V \equiv 0$ in Ω. Indeed, this is a standard argument in PDEs, because the system (2-20) can be proved to be strongly elliptic. Here, however, we use a more practical argument, by showing that this problem is equivalent to a classical boundary value problem in linear elasticity, for which well-known results hold. To this aim, we imagine that $U(x, y)$ and $V(x, y)$ represents the displacement field of a fictitious two-dimensional linear-elastic body Ω, with Young's modulus E and Poisson's ration ν, for which the (fictitious) stress components read

$$\hat{\sigma}_x=\frac{E}{1-\nu^2}(U_{,x}+\nu V_{,y}), \quad \hat{\sigma}_y=\frac{E}{1-\nu^2}(V_{,y}+\nu U_{,x}), \quad \hat{\sigma}_{xy}=\frac{E}{2(1+\nu)}(U_{,y}+V_{,x}). \tag{2-22}$$

It can then be shown that equations (2-20) with boundary conditions (2-21) can be rewritten as

$$\begin{cases}\hat{\sigma}_{x,x}+\hat{\sigma}_{xy,y}=0\\ \hat{\sigma}_{xy,x}+\hat{\sigma}_{y,y}=0\end{cases} \quad \text{in } \Omega, \tag{2-23}$$

$$\begin{cases}\hat{\sigma}_x n_x+\hat{\sigma}_{xy}n_y=0\\ \hat{\sigma}_{xy}n_x+\hat{\sigma}_y n_y=0\end{cases} \quad \text{on } \partial\Omega. \tag{2-24}$$

In the language of linear elasticity, these represent the equilibrium of a body in generalized plane stress with null boundary traction. Kirchhoff's theorem [Knops and Payne 1971] states that there is at most one solution to the Dirichlet boundary value problems in plane elasticity provided $-\infty < \nu < \frac{1}{2}$, $\nu \neq -1$, $E \neq 0$; in the traction boundary value problem there is uniqueness to within a rigid body displacement. In the considered case of null body forces and null boundary traction, since $E > 0$ and $-1 < \nu < \frac{1}{2}$, the solution is unique and it consist in a null stress field, leading to a displacement field of the form

$$\begin{pmatrix}U(x, y)\\ V(x, y)\end{pmatrix}=\begin{pmatrix}-\omega y\\ \omega x\end{pmatrix}+\begin{pmatrix}c_1\\ c_2\end{pmatrix}, \tag{2-25}$$

with constants c_1, c_2 and ω, that represents an infinitesimal rigid body displacement. It is easy to show that such constants are null for the case at hand if the laminated glass package is properly constraint in order to prevent its rigid displacements. In conclusion, one finds $U(x, y) \equiv 0$ and $V(x, y) \equiv 0$, for which the expected identities

$$u_2(x, y)=-\frac{h_1}{h_2}\,u_1(x, y), \quad v_2(x, y)=-\frac{h_1}{h_2}\,v_1(x, y). \tag{2-26}$$

This is because the in-plane forces in the two glass plies, which are due to the mutual shear forces transmitted by the interlayer, must balance one another.

2.4. ***Layered and monolithic limits.*** When the shear modulus of the interlayer vanishes, i.e., $G \to 0$, conditions (2-3), (2-4), (2-5), (2-6) and (2-7) take the form ($i = 1, 2$)

$$\begin{cases} (D_1 + D_2)\triangle\triangle w - p(x, y) = 0, \\ \dfrac{12D_i}{h_i^2}\Big(u_{i,xx} + \dfrac{1-\nu}{2}u_{i,yy} + \dfrac{1+\nu}{2}v_{i,xy}\Big) = 0, \\ \dfrac{12D_i}{h_i^2}\Big(v_{i,yy} + \dfrac{1-\nu}{2}v_{i,xx} + \dfrac{1+\nu}{2}u_{i,xy}\Big) = 0. \end{cases} \tag{2-27}$$

The first equation clearly corresponds to the flexural equilibrium of two frictionless sliding glass plates, with flexural bending $D_1 + D_2$, subject to a distributed load $p(x, y)$, while the others are the equilibrium conditions for the in-plane forces in x and y direction of the upper and lower glass plies, respectively. This is the *layered limit*, i.e., the laminated glass plate behaves as two free-sliding glass plies.

When $G \to +\infty$, then the shear strain in the interlayer tends to zero, i.e., $\tilde{\gamma}_{zx} = 0$, $\tilde{\gamma}_{zy} = 0$ in (2-1). Using the relationships (2-26), such conditions give:

$$\begin{aligned} &\tilde{\gamma}_{zx} = [u_1 - u_2 + w_{,x}\, H]/t = 0 \qquad \Rightarrow \quad u_1 = -\frac{D_2 h_1^2}{D_1 h_2^2 + D_2 h_1^2} H\, w_{,x} = -\frac{h_2}{h_1 + h_2} H\, w_{,x}\,, \\ &\tilde{\gamma}_{zy} = [v_1 - v_2 + w_{,y}\, H]/t = 0 \qquad \Rightarrow \quad v_1 = -\frac{D_2 h_1^2}{D_1 h_2^2 + D_2 h_1^2} H\, w_{,y} = -\frac{h_2}{h_1 + h_2} H\, w_{,y}\,. \end{aligned} \tag{2-28}$$

Substituting in the Euler–Lagrange equations, one finds

$$\begin{cases} D_{\text{tot}}\triangle\triangle w - p(x, y) = 0, \\ \dfrac{12D_1}{h_1^2}\Big(u_{1,xx} + \dfrac{1-\nu}{2}u_{1,yy} + \dfrac{1+\nu}{2}v_{1,xy}\Big) = -\dfrac{12D_2}{h_2^2}\Big(u_{2,xx} + \dfrac{1-\nu}{2}u_{2,yy} + \dfrac{1+\nu}{2}v_{2,xy}\Big), \\ \dfrac{12D_1}{h_1^2}\Big(v_{1,yy} + \dfrac{1-\nu}{2}v_{1,xx} + \dfrac{1+\nu}{2}u_{1,xy}\Big) = -\dfrac{12D_2}{h_2^2}\Big(v_{2,yy} + \dfrac{1-\nu}{2}v_{2,xx} + \dfrac{1+\nu}{2}u_{2,xy}\Big), \\ G\tilde{\gamma}_{zx} = \dfrac{12D_1}{h_1^2}\Big(u_{1,xx} + \dfrac{1-\nu}{2}u_{1,yy} + \dfrac{1+\nu}{2}v_{1,xy}\Big), \\ G\tilde{\gamma}_{zy} = \dfrac{12D_1}{h_1^2}\Big(v_{1,yy} + \dfrac{1-\nu}{2}v_{1,xx} + \dfrac{1+\nu}{2}u_{1,xy}\Big), \end{cases} \tag{2-29}$$

where the quantity D_{tot}, defined as

$$D_{\text{tot}} = D_1 + D_2 + \frac{12D_1 D_2}{D_1 h_2^2 + D_2 h_1^2} H^2 = D_1 + D_2 + \frac{E}{1-\nu^2}\frac{h_1 h_2}{h_1 + h_2} H^2, \tag{2-30}$$

represents the flexural stiffness of a monolithic plate, whose flexural inertia is that of the two glass plies properly spaced of the gap given by the thickness of the interlayer. This is indeed the *monolithic limit* of laminated glass [Bennison et al. 1999].

3. The enhanced effective thickness approach

It is not possible to solve the system of differential equations (2-3), (2-4), (2-5), (2-6) and (2-7) in closed form, but an approximation can be found by choosing an appropriate class of shape functions for the unknown fields $w(x, y)$, $u_1(x, y)$, $u_2(x, y)$, $v_1(x, y)$ and $v_2(x, y)$ defined up to parameters that will be

determined from energy minimization. The shape functions must be compatible with the qualitative properties of the exact solution and, in particular, must comprehend the monolithic-limit solution, when $G \to \infty$, and the layered-limit solution, when $G \to 0$. In terms of the field $w(x, y)$, such borderline cases correspond, respectively, to the fields $w_M(x, y)$ and $w_L(x, y)$ that, being the solutions of the differential equations

$$D_{\text{tot}} \triangle\triangle w_M(x, y) - p(x, y) = 0, \;\; (D_1 + D_2) \triangle\triangle w_L(x, y) - p(x, y) = 0, \tag{3-1}$$

are of the form

$$w_M(x, y) \equiv \frac{g(x, y)}{D_{\text{tot}}}, \;\; w_L(x, y) \equiv \frac{g(x, y)}{D_1 + D_2}, \tag{3-2}$$

where $g(x, y)$ is a function that depends upon the boundary conditions of the problem at hand. Henceforth, we may define the equivalent (reduced) flexural rigidity of the laminate plate

$$\frac{1}{D_R} = \frac{\eta}{D_{\text{tot}}} + \frac{1 - \eta}{D_1 + D_2}, \tag{3-3}$$

being the parameter η a nondimensional quantity, tuning the plate response from the layered limit ($\eta = 0$) to the monolithic limit ($\eta = 1$). An approximating class of solutions can thus be sought in the form

$$w(x, y) = \frac{g(x, y)}{D_R}, \tag{3-4}$$

where $g(x, y)$ is the shape function for the vertical displacement, uniquely determined by the shape of the laminated glass plate in $x - y$ plane, by the external load $p(x, y)$ and by the geometric boundary conditions.

The shape functions for the in-plane displacements should also guarantee that $\tilde{\gamma}_{zx} = 0$, $\tilde{\gamma}_{zy} = 0$ in the borderline monolithic case. Recalling (2-18) and (2-19), we select the form

$$\begin{aligned} u_1(x, y) &= -\beta \frac{1}{D_{\text{tot}}} \frac{h_2}{h_1 + h_2} H g_{,x}(x, y), \quad u_2(x, y) = \beta \frac{1}{D_{\text{tot}}} \frac{h_1}{h_1 + h_2} H g_{,x}(x, y), \\ v_1(x, y) &= -\beta \frac{1}{D_{\text{tot}}} \frac{h_2}{h_1 + h_2} H g_{,y}(x, y), \quad v_2(x, y) = \beta \frac{1}{D_{\text{tot}}} \frac{h_1}{h_1 + h_2} H g_{,y}(x, y), \end{aligned} \tag{3-5}$$

where β is another nondimensional parameter, again tuning the response from the layered limit ($\beta = 0$, implying null in-plane force in the glass layers) to the monolithic limit ($\beta = 1$, leading to $\tilde{\gamma}_{zx} = \tilde{\gamma}_{zy} = 0$).

The corresponding total strain energy (2-2) can thus be rewritten as a function of the parameters η and β to give

$$\begin{aligned} &\mathfrak{E}[w, u_1, u_2, v_1, v_2] = \widetilde{\mathfrak{E}}[\eta, \beta] = \\ &\frac{1}{2} \int_\Omega \left\{ \left(\frac{D_1 + D_2}{D_R^2} + \beta^2 \frac{12 D_1 D_2 H^2}{D_1 h_2^2 + D_2 h_1^2} \frac{1}{D_{\text{tot}}} \right) \left[(g_{,xx} + g_{,yy})^2 - 2(1 - \nu)(g_{,xx}\, g_{,yy} - g_{,xy}^2) \right] \right. \\ &\qquad \left. + \frac{G H^2}{t} \left(\frac{1}{D_R} - \frac{\beta}{D_{\text{tot}}} \right) [g_{,x}^2 + g_{,y}^2] + 2 \frac{p(x, y)}{D_R}\, g \right\} dx\, dy. \end{aligned} \tag{3-6}$$

This expression can be simplified by observing from (3-1) and (3-2) that $w(x, y) = g(x, y)/D_R$ of (3-4) is the exact solution of the elastic bending of a plate with constant flexural rigidity D_R under the load $p(x, y)$, with the same domain Ω and the geometric boundary condition of the problem at hand.

Consider the virtual work equality for this elastic body, in which the aforementioned $w(x, y)$ is selected as the strain/displacement field, whereas the stress/force field in equilibrium with $p(x, y)$ is given by

$$\begin{cases} M_x = -D_R(w_{,xx} + \nu w_{,yy}) = -(g_{,xx} + \nu g_{,yy}), \\ M_y = -D_R(w_{,yy} + \nu w_{,xx}) = -(g_{,yy} + \nu g_{,xx}), \\ M_{xy} = D_R(1-\nu) w_{,xy} = (1-\nu) g_{,xy}\,. \end{cases} \tag{3-7}$$

The external and internal virtual works, L_{ve} and L_{vi}, can be written as

$$\begin{aligned} L_{ve} &= -\frac{1}{D_R}\int_\Omega p(x, y)\, g\, dx\, dy, \\ L_{vi} &= \int_\Omega [M_x w_{,x} + M_y w_{,y} + M_{xy}\gamma_{xy}]\, dx\, dy \\ &= -\frac{1}{D_R}\int_\Omega \big[(g_{,xx} + g_{,yy})^2 - 2(1-\nu)(g_{,xx}\, g_{,yy} - g_{,xy}^2)\big]\, dx\, dy. \end{aligned} \tag{3-8}$$

Equality of external and internal virtual work then gives

$$\int_\Omega p(x, y) g\, dx\, dy = \int_\Omega \big[(g_{,xx} + g_{,yy})^2 - 2(1-\nu)(g_{,xx}\, g_{,yy} - g_{,xy}^2)\big]\, dx\, dy. \tag{3-9}$$

This condition allows a drastic simplification of the energy (3-6). In fact, substituting (3-9) into (3-6), the following expression for the strain energy can be found:

$$\begin{aligned} &\mathfrak{E}[w, u_1, u_2, v_1, v_2] = \widetilde{\mathfrak{E}}[\eta, \beta] = \\ &\frac{1}{2}\int_\Omega \left\{ \left(\frac{D_1 + D_2}{D_R^2} + \beta^2 \frac{12 D_1 D_2 H^2}{D_1 h_2^2 + D_2 h_1^2} \frac{1}{D_{\text{tot}}} \right) p(x, y)\, g \right. \\ &\qquad \left. + \frac{G H^2}{t}\left(\frac{1}{D_R} - \frac{\beta}{D_{\text{tot}}} \right)[g_{,x}^2 + g_{,y}^2] + \frac{p(x, y)\, g}{D_R} \right\} dx\, dy. \end{aligned} \tag{3-10}$$

Since $g(x, y)$ is supposed to have been determined from (3-1), the integral in (3-10) depends upon the free parameters η and β only, whose optimal value, say η^* and β^*, is obtained by direct minimization. The final result is that

$$\eta^* = \beta^* = \frac{1}{1 + \dfrac{D_1 + D_2}{(G/t) D_{\text{tot}}} \dfrac{12 D_1 D_2}{D_1 h_2^1 + D_2 h_1^2} \Psi}, \tag{3-11}$$

where the coefficient

$$\Psi = \frac{\int_\Omega p(x, y)\, g\, dx\, dy}{\int_\Omega [g_{,x}^2 + g_{,y}^2]\, dx\, dy} \tag{3-12}$$

depends upon the geometry of the plate and on its boundary and loading condition.

Deflection-effective thickness. The coefficient η, appearing in the definition of D_R (3-3), is in some sense analogous to the parameter Γ of (1-5) in the Bennison–Wölfel model [Wölfel 1987; Bennison 2009; Calderone et al. 2009], because the layered limit corresponds to $\Gamma = \eta = 0$ and the monolithic limit to $\Gamma = \eta = 1$. From (3-3), the *deflection-effective thickness* $\hat{h}_{\text{ef};w}$, associated with the value η^*, can be written in the form

$$\hat{h}_w = \left(\frac{\eta^*}{h_1^3 + h_2^3 + 12\dfrac{h_1 h_2}{h_1 + h_2} H^2} + \frac{1 - \eta^*}{h_1^3 + h_2^3} \right)^{-1/3}. \tag{3-13}$$

Stress-effective thickness. The stress-effective thickness may be defined as the (constant) thickness $\hat{h}_{i;\mathrm{ef};\sigma}$ of a monolithic plate for which the maximum bending stress is equal to the maximum stresses in the i-th glass layer of the laminated plate. The stresses in a monolithic plate are associated with the moments per-unit-length $M_x,\ M_y,\ M_{xy}$, defined by (3-7). On the other hand, the i-th glass ply of the laminated plate is subjected to moments and in-plane forces per unit length given by (2-13) and (2-11), respectively. Then, $\hat{h}_{i;\mathrm{ef};\sigma}$ can be found by equating the two contributions, i.e.,

$$\begin{aligned}
|\sigma_{xx}|_{\max} &= \max \left| \frac{N_{ix}(x, y)}{h_i} \pm \frac{6M_{ix}(x, y)}{h_i^2} \right| = \frac{\max |M_x(x, y)|}{\frac{1}{6}\hat{h}_{i;\mathrm{ef};\sigma}^2}, \\
|\sigma_{yy}|_{\max} &= \max \left| \frac{N_{iy}(x, y)}{h_i} \pm \frac{6M_{iy}(x, y)}{h_i^2} \right| = \frac{\max |M_y(x, y)|}{\frac{1}{6}\hat{h}_{i;\mathrm{ef};\sigma}^2}, \\
|\sigma_{xy}|_{\max} &= \max \left| \frac{N_{ixy}(x, y)}{h_i} \pm \frac{6M_{ixy}(x, y)}{h_i^2} \right| = \frac{\max |M_{xy}(x, y)|}{\frac{1}{6}\hat{h}_{i;\mathrm{ef};\sigma}^2}.
\end{aligned} \tag{3-14}$$

Recalling (3-4) and (3-5), the moments and in-plane forces per unit length can be rewritten as a function of the shape function $g(x, y)$ in the form

$$\begin{aligned}
M_{ix} &= -\frac{D_i}{D_R}(g_{,xx} + \nu g_{,yy}), \quad N_{ix} = -(-1)^i \eta^* \frac{12 D_1 D_2}{D_2 h_1^2 + D_1 h_2^2} \frac{H}{D_{\mathrm{tot}}}(g_{,xx} + \nu g_{,yy}), \\
M_{iy} &= -\frac{D_i}{D_R}(g_{,yy} + \nu g_{,xx}), \quad N_{iy} = -(-1)^i \eta^* \frac{12 D_1 D_2}{D_2 h_1^2 + D_1 h_2^2} \frac{H}{D_{\mathrm{tot}}}(g_{,yy} + \nu g_{,xx}), \\
M_{ixy} &= (1 - \nu)\frac{D_i}{D_R} g_{,xy}, \qquad N_{ixy} = -(-1)^i \eta^* (1 - \nu) \frac{12 D_1 D_2}{D_2 h_1^2 + D_1 h_2^2} \frac{H}{D_{\mathrm{tot}}} g_{,xy}.
\end{aligned} \tag{3-15}$$

After defining, as in [Bennison 2009],

$$h_{s;1} = \frac{h_1 H}{h_1 + h_2}, \quad h_{s;2} = \frac{h_2 H}{h_1 + h_2}, \tag{3-16}$$

one finds from (3-14) expressions analogous to that defined in (1-7) in the form

$$\frac{1}{\hat{h}_{1;\sigma}^2} = \frac{2\eta^* h_{s;2}}{h_1^3 + h_2^3 + 12\dfrac{h_1 h_2}{h_1 + h_2} H} + \frac{h_1}{\hat{h}_w^3}, \quad \frac{1}{\hat{h}_{2;\sigma}^2} = \frac{2\eta^* h_{s;1}}{h_1^3 + h_2^3 + 12\dfrac{h_1 h_2}{h_1 + h_2} H} + \frac{h_2}{\hat{h}_w^3}. \tag{3-17}$$

Notice that the expressions for the effective thickness (3-13) and (3-17) are of the same type obtained in [Galuppi and Royer-Carfagni 2012] for the one dimensional case.

In the following, the method based upon formulas (3-13) and (3-17) will be referred to as the enhanced effective thickness (EET) approach.

4. Examples

The four paradigmatic cases of rectangular laminated plates $\{0 \le x \le a;\ 0 \le y \le b\}$ with various boundary conditions, as shown in Figure 5, are now examined. We set $b = 2000\,\text{mm}$, while for a the three values $a = 2000\,\text{mm}$, $a = 3000\,\text{mm}$ and $a = 6000\,\text{mm}$ are considered. Parameters for glass plates are $E = 70\,\text{GPa}$, $\nu = 0.22$, $h_1 = h_2 = 10\,\text{mm}$, the thickness of the interlayer is $t = 0.76\,\text{mm}$ while its shear modulus G is continuously varied from 0.01 MPa to 10 MPa, in order to evaluate its influence on the shear-coupling of the glass plies. All the laminates are subjected to a uniformly distributed pressure $p = 0.75\,\text{kN/m}^2$, but since all materials are linear elastic, stress and strain depend linearly upon p. The results obtained with the approximate methods will in each case be compared with an accurate numerical analysis performed with ABAQUS, using a 3-D mesh with 110000 solid 20-node quadratic bricks with reduced integration, available in the ABAQUS program library.

The shape function $g(x, y)$ of (3-4) is assumed according to the form (uniform distribution) of the external load $p(x, y)$ and the geometric boundary conditions. The coefficient η^*, which allows to calculate the stress and deflection-effective thickness, as per (3-13) and (3-17), is calculated by using (3-11), evaluating the parameter Ψ through (3-12). But since for the case at hand $h_1 = h_2 = h$, as customary in the design practice, the expression for η^* can be simplified:

$$\eta^* = \frac{1}{1 + \dfrac{t}{G}\dfrac{E}{1-\nu^2}\dfrac{h^3}{2(h^2+3H^2)}\Psi}. \tag{4-1}$$

To facilitate the analysis of rectangular plates of any size, the values of Ψ are recorded in tables as a function of the length a and of the aspect ratio $\lambda = b/a$.

4.1. ***Simply supported rectangular plates.*** Consider a rectangular laminated glass under a uniformly distributed load p with four simply supported edges (Figure 5a). The classical Navier solution [Timoshenko and Woinowsky-Krieger 1971] gives the elastic deflection of a monolithic plate with flexural

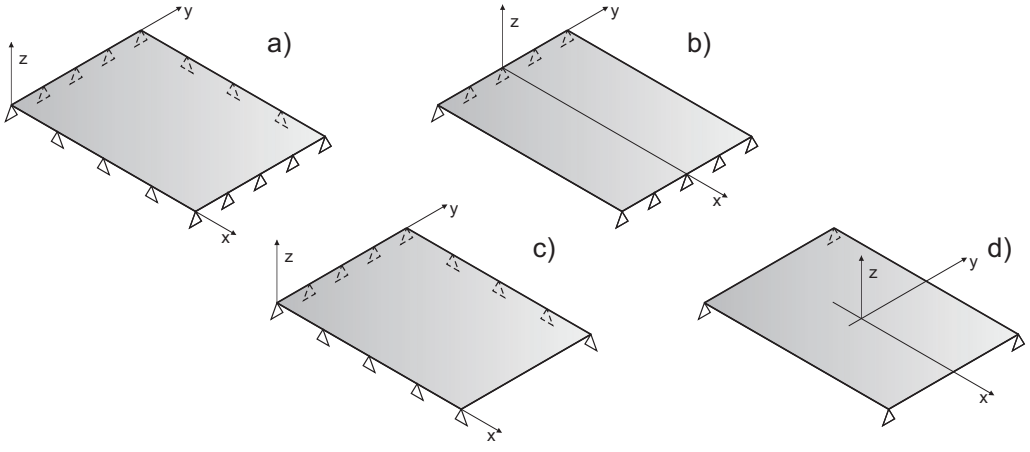

Figure 5. Representative examples of laminated glass plates under various boundary and load conditions.

a[mm] \ λ	0.1	0.2	0.3	0.4	0.5	0.6	0.7	0.8	0.9	1
500	39.8732	10.2644	4.7813	2.8622	1.9739	1.4914	1.2005	1.0116	0.8822	0.7896
1000	9.9683	2.5661	1.1953	0.7155	0.4935	0.3729	0.3001	0.2529	0.2205	0.1974
1500	4.4304	1.1405	0.5313	0.3180	0.2193	0.1657	0.1334	0.1124	0.0980	0.0877
2000	2.4921	0.6415	0.2988	0.1789	0.1234	0.0932	0.0750	0.0632	0.0551	0.0493
2500	1.5949	0.4106	0.1913	0.1145	0.0790	0.0597	0.0480	0.0405	0.0353	0.0316
3000	1.1076	0.2851	0.1328	0.0795	0.0548	0.0414	0.0333	0.0281	0.0245	0.0219

Table 1. Coefficient Ψ (in $\mathrm{mm}^{-2} \times 10^4$) for rectangular plates with four edges simply supported.

rigidity D_R in the form

$$w(x, y) = \frac{16p}{\pi^6 D_R} \sum_{m=1}^{\infty} \sum_{n=1}^{\infty} \frac{\sin \dfrac{m\pi x}{a} \sin \dfrac{n\pi y}{b}}{nm\left(\dfrac{m^2}{a^2} + \dfrac{n^2}{b^2}\right)^2}. \tag{4-2}$$

Partial sums of a finite number of terms of the series can be used as approximations of the entire function. By taking just the first term in the series (first-order approximation), the shape function $g(x, y)$ of (3-4) is

$$g(x, y) = \frac{16p}{\pi^6} \frac{1}{\left(\dfrac{1}{a^2} + \dfrac{1}{b^2}\right)^2} \sin \frac{\pi x}{a} \sin \frac{\pi y}{b}, \tag{4-3}$$

and the corresponding graph is drawn in Figure 6.

From this, the coefficient η^*, evaluated through (3-11) or (4-1), reads

$$\eta^* = \frac{1}{1 + \dfrac{D_1 + D_2}{(G/t) D_{\mathrm{tot}}} \dfrac{12 D_1 D_2}{D_1 h_2^1 + D_2 h_1^2} \dfrac{\pi^2 (a^2 + b^2)}{a^2 b^2}}. \tag{4-4}$$

It has been directly verified that higher-order approximations, obtained by considering more terms of the series (4-2), do not substantially increase the level of accuracy. The coefficient $\Psi[\mathrm{mm}^{-2}]$ that appears in (3-11) and (4-1) is tabulated in Table 1 as a function of the length a [mm] and of the aspect ratio $\lambda = b/a$.

For the case $a = 3000$ mm, $b = 2000$ mm and for a shear modulus of the polymeric interlayer G varying from 0, 01 MPa to 10 MPa, the graphs in Figure 7 compare the deflection- and stress-effective thickness

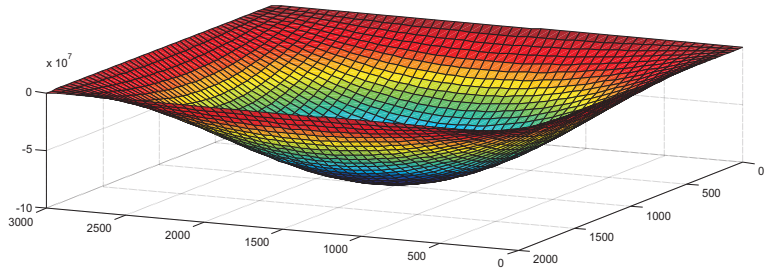

Figure 6. Shape function for simply supported rectangular laminated plates. Case $a =$ 3000 mm, $b = 2000$ mm.

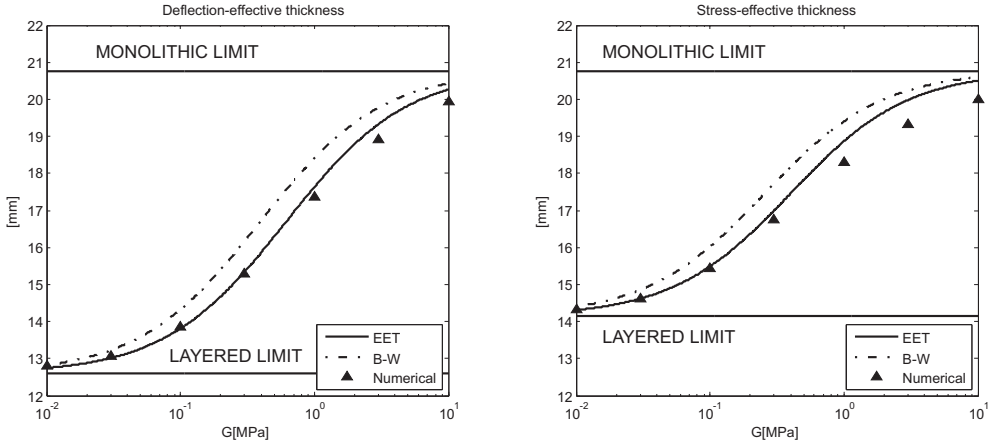

Figure 7. Simply supported rectangular plate, case $a = 3000\,\text{mm}$, $b = 2000\,\text{mm}$. Comparison of the effective thicknesses obtained with the Bennison–Wölfel approach (B-W), the enhanced effective thickness approach (ETT), and numerical simulations.

calculated according to the proposed approach of Section 3, here referred to as EET (enhanced effective thickness), with the effective thicknesses calculated through (1-6) and (1-7) for the Bennison–Wölfel model, recalled in the Introduction.

It is evident here that the proposed enhanced effective-thickness (ETT) approach and the Bennison–Wölfel (B-W) formulation give qualitatively different results. However, B-W is on the side of safeness, because it predicts deflection and stress values higher than those predicted by the EET approach. The numerical simulations show that the EET approach provides a better approximation than B-W, but the difference is not substantial, at least for the case at hand. The analytical approach recently proposed in [Foraboschi 2012] for the particular case at hand gives results in good agreement with the EET results.

The case of Figure 8 corresponds to $a = 6000\,\text{mm}$ and $b = 2000\,\text{mm}$, that is, the plate is a long rectangle whose deformation tends to be cylindrical in a neighborhood of the center. In such a case, the behavior predicted by the EET approach is close to Bennison–Wölfel's. This is not surprising because the aspect ratio is such that plate response is similar to the response of a beam ($\lambda = b/a \gg 1$), and Bennison–Wölfel's model is calibrated on the case of simply supported beams under uniformly distributed load [Galuppi and Royer-Carfagni 2012]. Numerical simulations confirm the accuracy.

On the contrary, the greatest differences between the EET and B-W approaches are obtained when the plate is square, i.e., when the deflections of beam and plate differ the most. This case is illustrated in Figure 9 for a plate with $a = 2000\,\text{mm}$ and $b = 2000\,\text{mm}$. It is evident, here, that the results achieved through the ETT approach are closer to the numerical data.

4.2. ***Rectangular plates with two opposite simply supported sides.*** For the case of rectangular plates with two opposite simply supported sides (Figure 5b), following [Timoshenko and Woinowsky-Krieger 1971] and reasoning as in the previous case, the shape function $g(x, y)$ may be chosen in the form

$$g(x, y) = pa^4 \sum_{m=1,3,5,\ldots}^{\infty} \left[\frac{4}{\pi^5 m^5} + A_m \cosh \frac{m\pi y}{a} + B_m \frac{m\pi y}{a} \sinh \frac{m\pi y}{a} \right] \sin \frac{m\pi x}{a}, \tag{4-5}$$

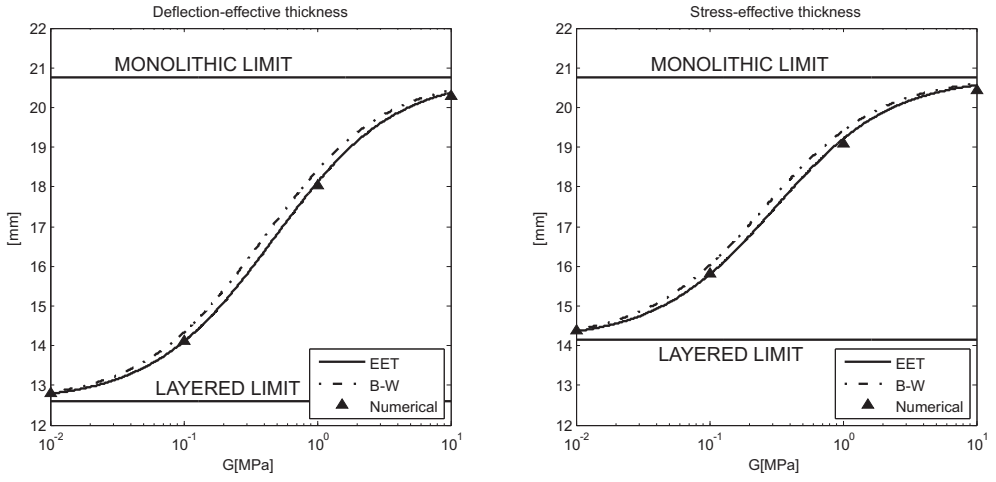

Figure 8. Simply supported rectangular plate, case $a = 6000\,\text{mm}$, $b = 2000\,\text{mm}$ (see Figure 7 for legend).

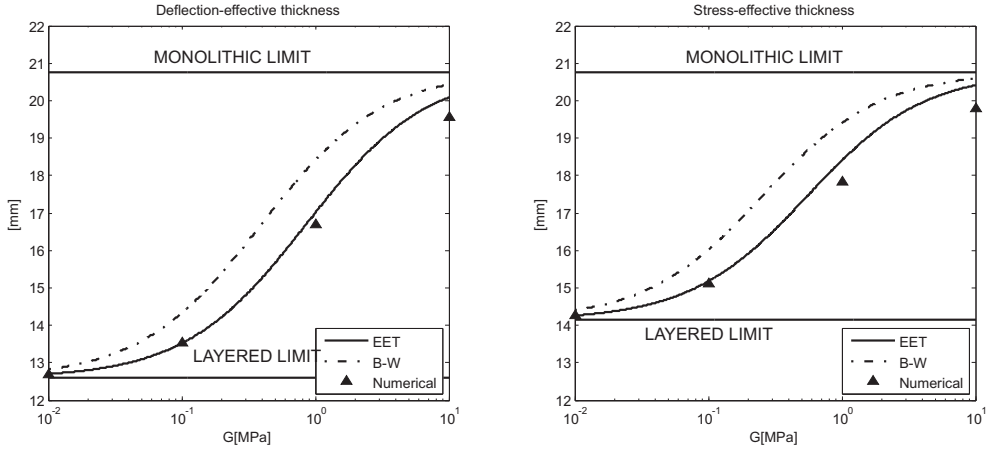

Figure 9. Simply supported square plate, case $a = 2000\,\text{mm}$, $b = 2000\,\text{mm}$ (see Figure 7 for legend).

where

$$A_m = \frac{4}{\pi^5 m^5} \frac{\nu(1+\nu)\sinh\frac{m\pi b}{2a} - \nu(1-\nu)\frac{m\pi b}{2a}\cosh\frac{m\pi b}{2a}}{(3+\nu)(1-\nu)\sinh\frac{m\pi b}{2a}\cosh\frac{m\pi b}{2a} - (1-\nu)^2\frac{m\pi b}{2a}},$$
$$B_m = \frac{4}{\pi^5 m^5} \frac{\nu(1-\nu)\sinh\frac{m\pi b}{2a}}{(3+\nu)(1-\nu)\sinh\frac{m\pi b}{2a}\cosh\frac{m\pi b}{2a} - (1-\nu)^2\frac{m\pi b}{2a}}. \tag{4-6}$$

We take a first-order approximation just keeping the first term of the series, whose graph is plotted in Figure 10.

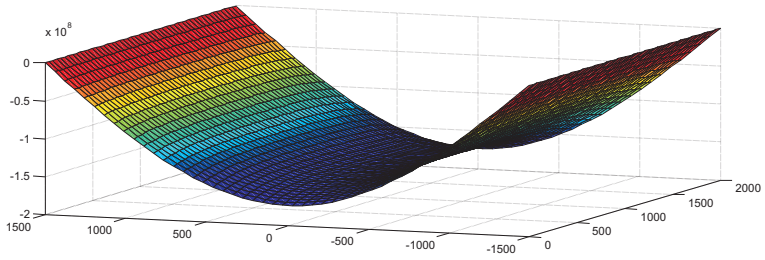

Figure 10. Shape function for rectangular plate with two opposite edges simply supported. Case $a = 3000\,\text{mm}$, $b = 2000\,\text{mm}$.

The coefficient η^* is given by (4-1), where Ψ, when evaluated by taking the first term only in the series, is of the form

$$\Psi = \frac{8\pi^2\big(4b + B_1\pi^5 bC + 2aS\pi^4(A_1 - B_1)\big)}{a\big(B_1^2\pi^{11}b^2SC + 32ab + abB_1(-B_1 + 4A_1S^2)\pi^{10} + 2a^2SC(2A_1^2 + B_1^2)\pi^9 + 16B_1\pi^5 abC + 32a^2S\pi^4(A_1 - B_1)\big)}, \tag{4-7}$$

with $C = \cosh\dfrac{m\pi b}{2a}$ and $S = \sinh\dfrac{m\pi b}{2a}$. The value of Ψ is reported in Table 2 as a function of a and $\lambda = b/a$.

Figure 11 shows the comparison between the deflection- and stress-effective thicknesses, calculated according to the enhanced effective thickness approach and to Bennison–Wölfel model as a function of G.

In this case the EET and B-W approaches give results that in practice coincide. A plate under these particular boundary conditions presents in fact a cylindrical deformed shape very similar to that of a beam with equivalent cross-sectional inertia. The good approximation that can be achieved is evidenced by the comparison with the numerical results.

4.3. ***Rectangular plates with three simply supported sides.*** For the case of rectangular plates with three simply supported sides under uniform pressure (Figure 5c), Timoshenko and Woinowsky-Krieger [1971] furnishes the general form for the elastic deflection of a monolith. Then, the shape function can be

a[mm] \ λ	0.2	0.4	0.6	0.8	1	1.25	1.667	2.5	5
500	0.4233	0.3908	0.3816	0.3770	0.3742	0.3718	0.3690	0.3653	0.3579
1000	0.1058	0.0977	0.0954	0.0943	0.0935	0.0929	0.0922	0.0913	0.0895
1500	0.0470	0.0434	0.0424	0.0419	0.0416	0.0413	0.0410	0.0406	0.0398
2000	0.0265	0.0244	0.0238	0.0236	0.0234	0.0232	0.0231	0.0228	0.0224
2500	0.0169	0.0156	0.0153	0.0151	0.0150	0.0149	0.0148	0.0146	0.0143
3000	0.0118	0.0109	0.0106	0.0105	0.0104	0.0103	0.0102	0.0101	0.0099

Table 2. Coefficient Ψ (in $\text{mm}^{-2} \times 10^4$) for rectangular plates with two opposite edges simply supported.

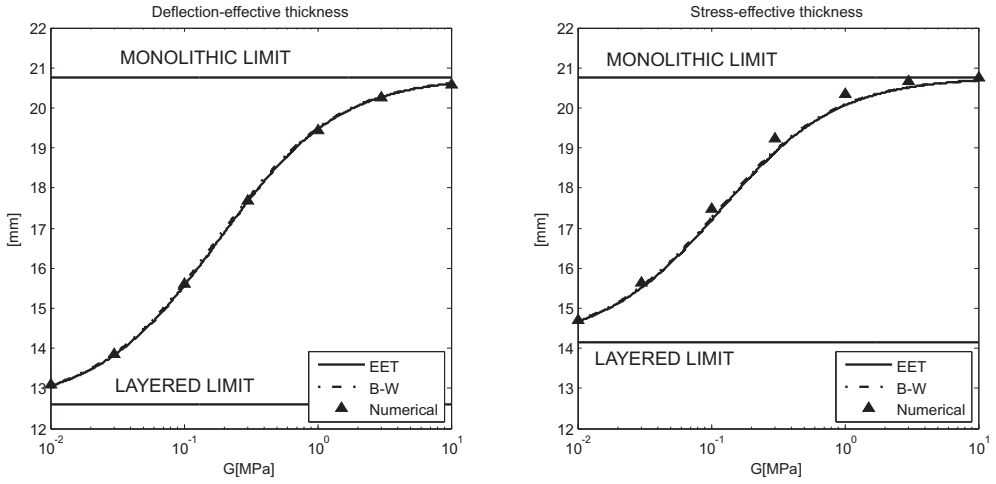

Figure 11. Rectangular plates with two opposite edges simply supported, case $a = 3000\,\text{mm}$, $b = 2000\,\text{mm}$. Comparison of the effective thicknesses obtained with: Bennison–Wölfel approach (B-W); the enhanced effective thickness approach (EET); the numerical simulations.

written as

$$g(x, y) = p\,a^4 \tag{4-8}$$
$$\times \sum_{m=1,3,5,\ldots}^{\infty} \left[\frac{4}{\pi^5 m^5} + A_m \cosh\frac{m\pi y}{a} + B_m \frac{m\pi y}{a} \sinh\frac{m\pi y}{a} + C_m \sinh\frac{m\pi y}{a} + D_m \frac{m\pi y}{a} \cosh\frac{m\pi y}{a} \right] \sin\frac{m\pi x}{a}$$

By imposing the relevant boundary conditions, one finds with some effort the values of the constants appearing in (4-8) in the form

$$\begin{gathered} A_m = -\frac{4}{\pi^5 m^5}, \quad B_m = \frac{2}{\pi^5 m^5}, \quad D_m = \frac{(2((3-\nu)S^2 + 2\nu C(C-1)))a}{((3+\nu)CSa + (1-\nu)\pi bm)\pi^5 m^5}, \\ C_m = \frac{2(\pi^2 m^2 (1-\nu)^2 b^2 + 2\nu(1-\nu)m\pi Sab + (2\nu C(C-1)(1+\nu) - 2S^2(3-\nu))a^2)}{(1-\nu)((3+\nu)CSa + (1-\nu)\pi bm)\pi^5 m^5 a}, \end{gathered} \tag{4-9}$$

where $C = \cosh(m\pi b/a)$ and $S = \sinh(m\pi b/a)$. Figure 12 shows the graph of the first-order approximation of the shape function. The coefficient Ψ to calculate η^* from (3-12) is tabulated in Table 3 again as a function of a and $\lambda = b/a$.

It is evident, from Figure 13, that the enhanced effective thickness approach and the Bennison–Wölfel model give, in the case at hands, slightly different results; the data obtained numerically are in favor of the approach proposed here.

4.4. ***Rectangular plates resting on corner points.*** The case of rectangular plates point-wise supported at the corners under uniform pressure (Figure 5d) is of particular interest for frameless glazing, but presents some difficulty because even the elastic solution for the monolith is not simple. The first attempts of analytical solutions were given by Galerkin [1915] and Nádai [1922]. Then Wang et al. [2002] proved

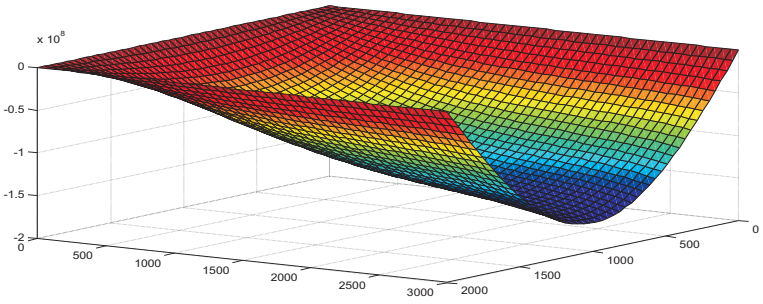

Figure 12. Shape function for rectangular plates with three simply supported sides. Case $a = 3000\,\text{mm}$, $b = 2000\,\text{mm}$.

a[mm] \ λ	0.2	0.4	0.6	0.8	1	1.25	1.667	2.5	5
500	0.5982	0.5578	0.5168	0.4855	0.4640	0.4465	0.4300	0.4156	0.4166
1000	0.1495	0.1394	0.1292	0.1214	0.1160	0.1116	0.1075	0.1039	0.1041
1500	0.0665	0.0620	0.0574	0.0539	0.0516	0.0496	0.0478	0.0462	0.0441
2000	0.0374	0.0349	0.0323	0.0303	0.0290	0.0279	0.0269	0.0260	0.0260
2500	0.0239	0.0223	0.0207	0.0194	0.0186	0.0179	0.0172	0.0166	0.0171
3000	0.0166	0.0155	0.0144	0.0135	0.0129	0.0124	0.0119	0.0115	0.0110

Table 3. Coefficient Ψ (in $\text{mm}^{-2} \times 10^4$) for rectangular plates with three edges simply supported.

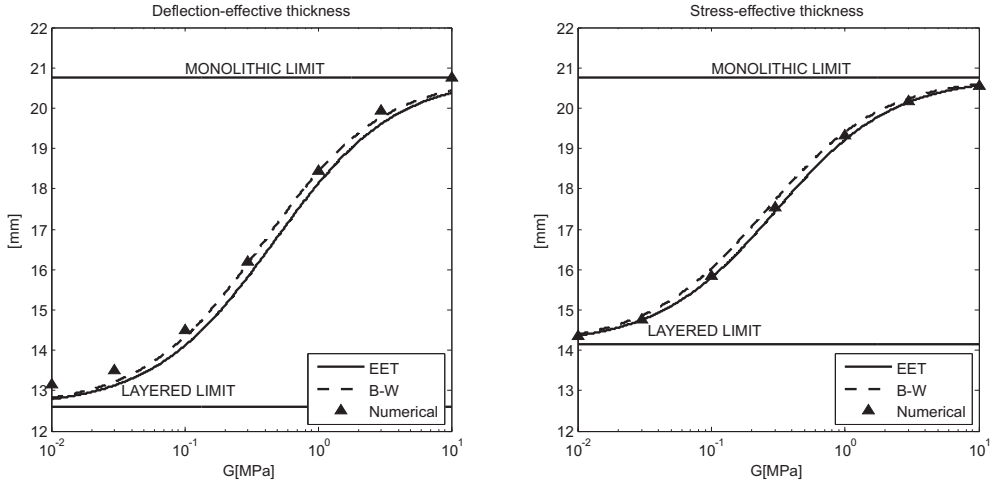

Figure 13. Rectangular plates with three simply supported edges, case $a = 3000\,\text{mm}$, $b = 2000\,\text{mm}$. Comparison of the effective thicknesses obtained with: Bennison–Wölfel approach (B-W); the enhanced effective thickness approach (EET); the numerical simulations.

that such works, focused on determining the deflection, produce rather inaccurate results in terms of stress. Batista [2010] presented a solution in form of trigonometric series , where the coefficients of the series form a regular *infinite* system of linear equations, providing accurate results for deflection, moment

and shear forces. Therefore, following Batista, the deflection of a monolith of flexural stiffness D is here expressed in the form

$$\begin{aligned} w(x,y) = {} & \frac{p}{48(1-\nu)D}\big[5(a^4+b^4) - 6\nu a^2b^2 - 6(a^2-\nu b^2)x^2 - 6(b^2-\nu a^2)y^2 + x^4 - 6\nu x^2y^2 + y^4\big] \\ & + \frac{p}{D}\sum_{n=0}^{\infty}(-1)^n B_n\Big[\Big(\frac{\sinh(\alpha_n b)}{\cosh(\alpha_n b)} + \frac{2}{(1-\nu)\alpha_n b}\Big)b\cosh(\alpha_n y) - y\sinh(\alpha_n y)\Big]\frac{\cos(\alpha_n x)}{a\cosh(\alpha_n b)} \\ & + \frac{p}{D}\sum_{n=0}^{\infty}(-1)^n D_n\Big[\Big(\frac{\sinh(\beta_n a)}{\cosh(\beta_n a)} + \frac{2}{(1-\nu)\beta_n a}\Big)a\cosh(\beta_n y) - x\sinh(\beta_n y)\Big]\frac{\cos(\beta_n y)}{b\cosh(\beta_n a)}, \end{aligned} \tag{4-10}$$

where $\alpha_n = (2n+1)\pi/(2a)$ and $\beta_n = (2n+1)\pi/(2b)$. The coefficients B_n and D_n can be found by expanding into a trigonometric series the boundary condition of null vertical forces on the free edges. By taking, as in the previous cases, just the first-order approximation, the shape function $g(x, y)$ reads

$$\begin{aligned} g(x,y) = {} & \frac{p}{48(1-\nu)}\big[5(a^4+b^4) - 6\nu a^2b^2 - 6(a^2-\nu b^2)x^2 - 6(b^2-\nu a^2)y^2 + x^4 - 6\nu x^2y^2 + y^4\big] \\ & + pB_0\Big[\Big(\frac{\sinh(\alpha_0 b)}{\cosh(\alpha_0 b)} + \frac{2}{(1-\nu)\alpha_0 b}\Big)b\cosh(\alpha_0 y) - y\sinh(\alpha_0 y)\Big]\frac{\cos(\alpha_0 x)}{a\cosh(\alpha_0 b)} \\ & + pD_0\Big[\Big(\frac{\sinh(\beta_0 a)}{\cosh(\beta_0 a)} + \frac{2}{(1-\nu)\beta_0 a}\Big)a\cosh(\beta_0 y) - x\sinh(\beta_0 y)\Big]\frac{\cos(\beta_0 y)}{b\cosh(\beta_0 a)}, \end{aligned} \tag{4-11}$$

where the coefficients B_0 and D_0 are given by

$$\begin{aligned} B_0 &= 16a^4b\ C_{ba}^2(1-\nu)\Big[-a(1-\nu)\pi^2 + 2b\ S_{ab}C_{ab}(3+\nu)\pi + \frac{16ab^4}{(b^2+a^2)^2}C_{ab}^2(1-\nu)\Big]\Big/Q, \\ D_0 &= 16a^4b\ C_{ba}^2(1-\nu)\Big[-b(1-\nu)\pi^2 + 2a\ S_{ba}C_{ba}(3+\nu)\pi + \frac{16a^4b}{(b^2+a^2)^2}\ C_{ba}^2(1-\nu)\Big]\Big/Q, \end{aligned} \tag{4-12}$$

with

$$\begin{aligned} Q = {} & \pi^2(ab(1-\nu)^2\pi^4 - 2(3+\nu)(1-\nu)(C_{ba}S_{ba}\,a^2 + S_{ab}C_{ab}\,b^2)\pi^3 \\ & + 4ab\ S_{ab}S_{ba}C_{ba}C_{ab}(3+\nu)^2\pi^2 - \frac{256a^5b^5}{(b^2+a^2)^4}\ C_{ab}^2C_{ba}^2(1-\nu)^2), \end{aligned}$$

$$C_{ab} = \cosh^2(\alpha_0 b), \quad S_{ab} = \sinh^2(\alpha_0 b), \quad C_{ba} = \cosh(\beta_0 a), \quad S_{ba} = \sinh(\beta_0 a). \tag{4-13}$$

The shape function thus obtained is plotted in Figure 14.

The coefficient η^* may be determined through (3-11) or (4-1) as a function of the material properties and of the coefficient Ψ of (3-12), tabulated in Table 4.

Figure 15 shows the comparison between the deflection- and stress-effective thickness calculated according to EET and B-W approaches, for the case $a = 3000$ mm, $b = 2000$ mm. From this, it is evident that the EET and B-W give substantially different results. For what concerns the stress-effective thickness, numerical experiments are in favor of our present proposal.

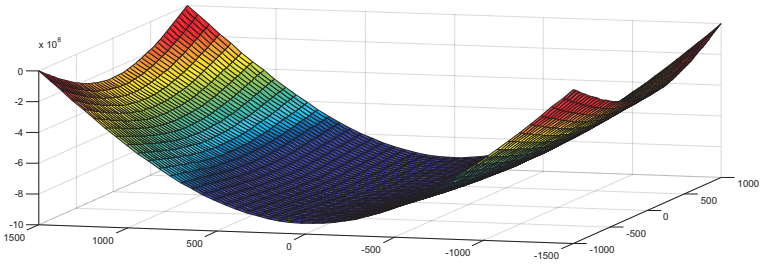

Figure 14. Shape function for rectangular plates resting on corner points. Case $a = 3000\,\text{mm}$, $b = 2000\,\text{mm}$.

a[mm] \ λ	0.1	0.2	0.3	0.4	0.5	0.6	0.7	0.8	0.9	1
500	0.6112	0.5982	0.5793	0.5578	0.5363	0.5168	0.4998	0.4855	0.4737	0.4640
1000	0.1528	0.1495	0.1448	0.1394	0.1341	0.1292	0.1249	0.1214	0.1184	0.1160
1500	0.0679	0.0665	0.0644	0.0620	0.0596	0.0574	0.0555	0.0539	0.0526	0.0516
2000	0.0382	0.0374	0.0362	0.0349	0.0335	0.0323	0.0312	0.0303	0.0296	0.0290
2500	0.0244	0.0239	0.0232	0.0223	0.0215	0.0207	0.0200	0.0194	0.0189	0.0186
3000	0.0170	0.0166	0.0161	0.0155	0.0149	0.0144	0.0139	0.0135	0.0132	0.0129

Table 4. Coefficient Ψ (in $\text{mm}^{-2} \times 10^4$) for rectangular plates resting on corner points.

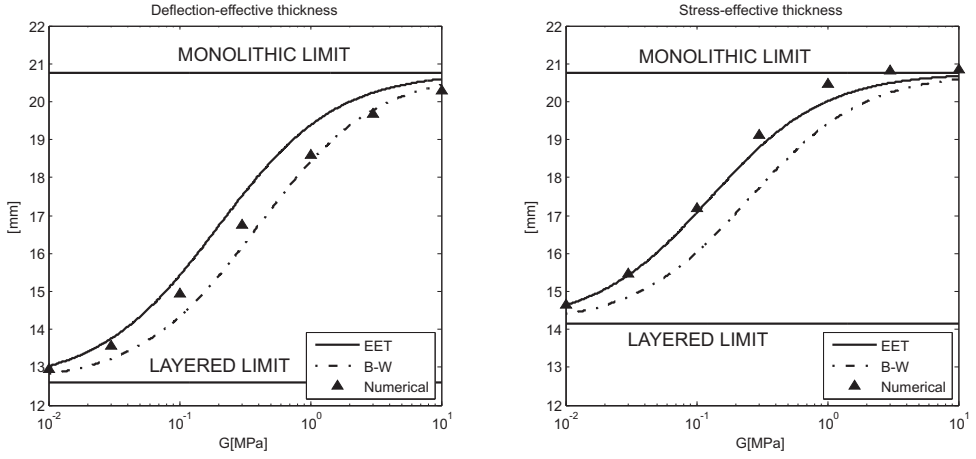

Figure 15. Rectangular plates supported at corner points, case $a = 3000\,\text{mm}$, $b = 2000\,\text{mm}$. Comparison of the effective thicknesses obtained with: Bennison–Wölfel approach (B-W); the enhanced effective thickness approach (EET); the numerical simulations.

Figure 16 shows the deflection- and stress-effective thickness for a $2000\,\text{mm} \times 2000\,\text{mm}$ square plate supported on corner points. Once again, in this case experimental results are better fitted through the EET approach.

Whenever $b \gg a$, the plate deformed shape tends to be cylindrical and, consequently, the behavior close to that of a beam. This is why for the case $a = 6000\,\text{mm}$ and $b = 2000\,\text{mm}$, recorded in Figure 17, B-W and EET give results that in practice coincide, in agreement with the numerical simulations.

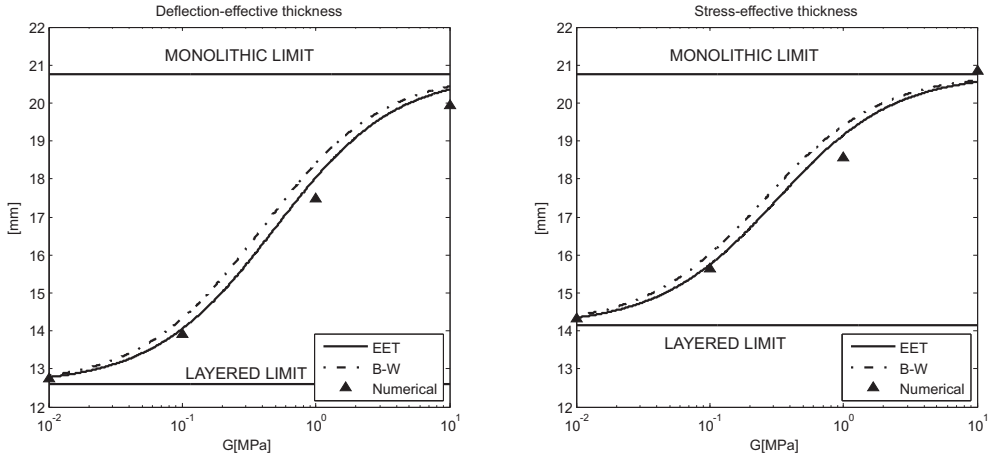

Figure 16. Square plates supported at corner points, case $a = 2000\,\text{mm}$, $b = 2000\,\text{mm}$. Comparison of the effective thicknesses obtained with: Bennison–Wölfel approach (B-W); the enhanced effective thickness approach (EET); the numerical simulations.

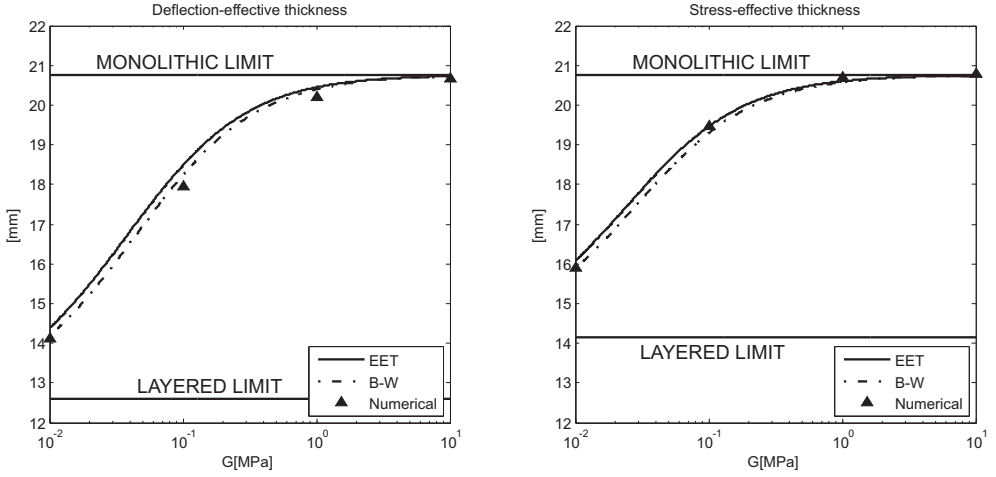

Figure 17. Rectangular plates supported at corner points, case $a = 6000\,\text{mm}$, $b = 2000\,\text{mm}$. Comparison of the effective thicknesses obtained with: Bennison–Wölfel approach (B-W); the enhanced effective thickness approach (EET); the numerical simulations.

5. Discussion and conclusions

Although it is possible to calculate numerically, and with excellent precision, the state of strain and stress in laminated glass of any composition, size and shape, under the most various boundary and load conditions, nevertheless simplified methods based upon the notion of effective thickness still remain a very powerful tool, especially in the first preliminary phases of the design procedure. The designers need simple expressions that allow to readily determine the structural response of laminated glass, leaving

more sophisticated computer methods to the final verifications. The most important result of this study has been the definition of simple formulas for the effective thickness that can be applied, in principle, to the two-dimensional problems of plates of any shape and size, under any boundary and load conditions. This method is not recommended to evaluate local effects, such as stress concentrations around holes and/or at contact points, but can be conveniently used to calculate maximum deflection and stress with good accuracy, as confirmed by numerical and analytical approaches [Foraboschi 2012].

The key point is the assumption of a shape-function $g(x, y)$ for the flexural-deformation surface of the laminate, which, in accord with (3-4), is taken equal to the deflection of a monolithic plate of arbitrary thickness with equal boundary and load conditions. Such a shape function may be estimated analytically, when an analytical though approximate solution is available, or even numerically, when this is not the case. From this, one can define the *deflection-* and *stress-effective thicknesses* of the laminate, by using the simple formulas (3-13) and (3-17). These are defined by a parameter η^*, indicating the shear coupling offered by the polymeric interlayer, whose form can be calculated from expression (3-11), which in turn is defined by the parameter Ψ, given by (3-12) as a function of the pressure distribution on the plate, $p(x, y)$, and of the shape function $g(x, y)$. Indeed, the only "difficulty" of the proposed method, here referred to as the enhanced effective thickness approach (EET), consists in calculating Ψ from (3-12), which involves integration of $p(x, y)$ and $g(x, y)$ over the referential domain of the plate, in accord with (3-12). Here, we have exemplified this procedure for the case, very important in the design practice, of a rectangular laminated glass plates under uniformly distributed pressure.

The shape function $g(x, y)$ has been approximated by the first term of the series expansion for the deflection surface of a monolithic plate, arriving at simple expressions for Ψ, whose values have been recorded in the tables of figures 1, 2, 3 and 4 for various boundary conditions at the borders. Comparisons with the results obtained with the classical formulas for the effective thickness *à la* Bennison–Wölfel (B-W), in accordance with (1-5), (1-6) and (1-7), and with the results from accurate numerical models, highlight the better accuracy that is obtained with the proposed EET approach. Indeed, the B-W approach assumes that laminated glass is a simply supported beam under uniformly distributed load; it then turns out to be reliable only when the flexural deformation of the plate is cylindrical, i.e., in the case of rectangular plates simply supported at two opposite sides. We have also shown that the use of B-W formulation is not always on the side of safeness because they are cases, like that of a laminated plate point-wise supported at the corners, where B-W gives effective thicknesses that underestimate both deflection and stress.

A more general and comprehensive treatment of other relevant problems for laminated glass design has been recorded in [Galuppi et al. 2012]. Here, the EET method is applied to the most common cases of the design practice including plates under pseudoconcentrated loads, providing synthetic tables for ease of reference and immediate applicability. The extension of the enhanced effective thickness approach to other cases, like that of curved plates and shells, presents in principle no further conceptual difficulty, and it will be the subject of future work.

Acknowledgements

Gianni Royer-Carfagni acknowledges the Italian MURST for its partial support under the PRIN2008 program.

References

[Aşik 2003] M. Z. Aşik, "Laminated glass plates: revealing of nonlinear behavior", *Comput. Struct.* **81**:28–29 (2003), 2659–2671.

[Aşik and Tezcan 2005] M. Z. Aşik and S. Tezcan, "A mathematical model for the behavior of laminated glass beams", *Comput. Struct.* **83**:21–22 (2005), 1742–1753.

[Batista 2010] M. Batista, "New analytical solution for bending problem of uniformly loaded rectangular plate supported on corner point", *IES J. A Civ. Struct. Eng.* **3**:2 (2010), 75–84.

[Behr et al. 1993] R. A. Behr, J. E. Minor, and H. S. Norville, "Structural behavior of architectural laminated glass", *J. Struct. Eng.* (*ASCE*) **119**:1 (1993), 202–222.

[Bennison 2009] S. J. Bennison, "Structural properties of laminated glass", short course presented at *Glass performance days* (Tampere), 2009.

[Bennison et al. 1999] S. J. Bennison, A. Jagota, and C. A. Smith, "Fracture of glass/poly(vinyl butyral) (Butacite®) laminates in biaxial flexure", *J. Am. Ceram. Soc.* **82**:7 (1999), 1761–1770.

[Bennison et al. 2001] S. J. Bennison, C. A. Smith, A. Van Duser, and A. Jagota, "Structural performance of laminated glass made with a 'stiff' interlayer", pp. 283–287 in *Glass processing days* (Tampere, 2001), edited by J. Vitkala, Tamglass, Tampere, 2001.

[Bennison et al. 2005] S. J. Bennison, J. G. Sloan, D. F. Kristunas, P. J. Buehler, T. Amos, and C. A. Smith, "Laminated glass for blast mitigation: role of interlayer properties", in *Glass processing days* (Tampere, 2005), Glaston Finland/GPD, Tampere, 2005.

[Bennison et al. 2008] S. J. Bennison, M. H. X. Qin, and P. S. Davies, "High-performance laminated glass for structurally efficient glazing", paper presented at conference on *Innovative light-weight structures and sustainable facades* (Hong Kong), 2008, available at http://tinyurl.com/Bennison-et-al-2008.

[Calderone et al. 2009] I. Calderone, P. S. Davies, S. J. Bennison, X. Huang, and L. Gang, "Effective laminate thickness for the design of laminated glass", in *Glass performance days* (Tampere, 2009), Glaston Finland/GPD, Tampere, 2009.

[Cas et al. 2007] B. Cas, M. Saje, and I. Planinc, "Buckling of layered wood columns", *Adv. Eng. Softw.* **38**:8–9 (2007), 586–597.

[Foraboschi 2007] P. Foraboschi, "Behavior and failure strength of laminated glass beams", *J. Eng. Mech.* (*ASCE*) **133**:12 (2007), 1290–1301.

[Foraboschi 2012] P. Foraboschi, "Analytical model for laminated-glass plate", *Compos. B Eng.* **43**:5 (2012), 2094–2106.

[Galerkin 1915] B. G. Galerkin, "Стержин и пластинки: ряды в некоторых волросах упругого равновесия стержней и пластинок", *Vestn. Inzh. Tekh.* (*USSR*) **1**:19 (1915), 897–908. In Russian; translated as *Rods and plates: series in some questions of elastic equilibrium of rods and plates*, National Technical Information Service, Springfield, VA, 1968.

[Galuppi and Royer-Carfagni 2012] L. Galuppi and G. F. Royer-Carfagni, "Effective thickness of laminated glass beams: new expressions via a variational approach", *Eng. Struct.* **38** (2012), 53–67.

[Galuppi et al. 2012] L. Galuppi, G. Manara, and G. F. Royer-Carfagni, "Practical expressions for the design of laminated glass", 2012, available at http://hdl.handle.net/1889/1720.

[Hooper 1973] J. A. Hooper, "On the bending of architectural laminated glass", *Int. J. Mech. Sci.* **15**:4 (1973), 309–323.

[Ivanov 2006] I. V. Ivanov, "Analysis, modelling, and optimization of laminated glasses as plane beam", *Int. J. Solids Struct.* **43**:22-23 (2006), 6887–6907.

[Knops and Payne 1971] R. J. Knops and L. E. Payne, *Uniqueness theorems in linear elasticity*, Springer, New York, 1971.

[Le Grognec et al. 2012] P. Le Grognec, Q.-H. Nguyen, and M. Hjiaj, "Exact buckling solution for two-layer Timoshenko beams with interlayer slip", *Int. J. Solids Struct.* **49**:1 (2012), 143–150.

[Louter et al. 2010] C. Louter, J. Belis, F. Bos, D. Callewaert, and F. Veer, "Experimental investigation of the temperature effect on the structural response of SG-laminated reinforced glass beams", *Eng. Struct.* **32**:6 (2010), 1590–1599.

[Murakami 1984] H. Murakami, "A laminated beam theory with interlayer slip", *J. Appl. Mech.* (*ASME*) **51**:3 (1984), 551–559.

[Nádai 1922] A. Nádai, "Über die Biegung durchlaufender Platten und der rechteckigen Platte mit freien Rändern", *Z. Angew. Math. Mech.* **2**:1 (1922), 1–26.

[Newmark et al. 1951] N. M. Newmark, C. P. Siess, and I. M. Viest, "Test and analysis of composite beams with incomplete interaction", *Proc. Soc. Exp. Stress Anal.* **9**:1 (1951), 75–92.

[Norville et al. 1998] H. S. Norville, K. W. King, and J. L. Swofford, "Behavior and strength of laminated glass", *J. Eng. Mech.* (*ASCE*) **124**:1 (1998), 46–53.

[Sagan 1969] H. Sagan, *Introduction to the calculus of variations*, McGraw-Hill, New York, 1969. Reprinted Dover, New York, 1992.

[Schnabl and Planinc 2011] S. Schnabl and I. Planinc, "The effect of transverse shear deformation on the buckling of two-layer composite columns with interlayer slip", *Int. J. Non-Linear Mech.* **46**:3 (2011), 543–553.

[Timoshenko and Woinowsky-Krieger 1971] S. P. Timoshenko and S. Woinowsky-Krieger, *Theory of plates and shells*, McGraw-Hill, New York, 1971.

[Wang et al. 2002] C. M. Wang, Y. C. Wang, and J. N. Reddy, "Problems and remedy for the Ritz method in determining stress resultants of corner supported rectangular plates", *Comput. Struct.* **80**:2 (2002), 145–154.

[Wölfel 1987] E. Wölfel, "Nachgiebiger Verbund: eine Näherungslösung und deren Anwendungsmöglichkeiten", *Stahlbau* **56**:6 (1987), 173–180.

[Xu and Wu 2007] R. Xu and Y. Wu, "Static, dynamic, and buckling analysis of partial interaction composite members using Timoshenko's beam theory", *Int. J. Mech. Sci.* **49**:10 (2007), 1139–1155.

Received 30 Nov 2011. Revised 1 Mar 2012. Accepted 16 Mar 2012.

LAURA GALUPPI: laura.galuppi@unipr.it
Civil-Environmental Engineering and Architecture, University of Parma, Parco Area delle Scienze 181/A, I, 43124 Parma, Italy

GIANNI ROYER-CARFAGNI: gianni.royer@unipr.it
Civil-Environmental Engineering and Architecture, University of Parma, Parco Area delle Scienze 181/A, I, 43124 Parma, Italy

JOURNAL OF MECHANICS OF MATERIALS AND STRUCTURES

jomms.net

Founded by Charles R. Steele and Marie-Louise Steele

See http://jomms.net for submission guidelines.

JoMMS (ISSN 1559-3959) is published in 10 issues a year. The subscription price for 2012 is US $555/year for the electronic version, and $735/year (+$60 shipping outside the US) for print and electronic. Subscriptions, requests for back issues, and changes of address should be sent to Mathematical Sciences Publishers, Department of Mathematics, University of California, Berkeley, CA 94720–3840.

JoMMS peer-review and production is managed by EditFLOW® from Mathematical Sciences Publishers.

PUBLISHED BY
mathematical sciences publishers
http://msp.org/

A NON-PROFIT CORPORATION

Typeset in LaTeX

Journal of Mechanics of Materials and Structures

Volume 7, No. 4 April 2012

1559-3959(2012)7:4;1-A